

RF DESIGN OF TRAVELING-WAVE ACCELERATING STRUCTURES FOR THE FCC-ee PRE-INJECTOR COMPLEX

H. W. Pommerenke*, A. Grudiev, A. Latina, CERN, Geneva, Switzerland
S. Bettoni, P. Craievich, J.-Y. Raguin, M. Schär, Paul Scherrer Institut, Villigen, Switzerland

Abstract

The linacs of the FCC-ee (Future Circular Electron-Positron Collider) injector complex will provide the drive beam for positron production and accelerate nominal electron and positron beams up to 6 GeV. Several linacs comprise different traveling-wave (TW) accelerating structures fulfilling the beam dynamics and rf constraints. Notably, high-phase advance large-aperture structures accelerate the positron beam at low energies. All TW structures are rotationally symmetric for easier production. Long-range wakes are damped by HOM detuning. Operating mode and HOM parameters were calculated based on lookup tables and analytic formulas, allowing for rapid scanning of large parameter spaces. In this paper, we present both methodology and realization of the rf design of the TW structures including their pulse compressors.

INTRODUCTION

The FCC-ee Conceptual Design Report (CDR) [1] considers a 6 GeV linac with 2 bunches per rf pulse at a repetition rate up to 200 Hz as baseline option for the FCC-ee injector complex. The bunches will have a charge of 5 nC each with an rms length of 1 mm or more and a spacing between 15 ns and 100 ns. The latest layout is shown in Fig. 1. Two separate linacs for electrons and positrons are foreseen up to 1.54 GeV. Both beams are then accelerated by the common linac to 6 GeV. To match the proposed filling scheme, the two low-energy linacs have to work at a repetition rate of 200 Hz and the common linac at 400 Hz, 200 Hz each for positrons and electrons [1, 2].

Over the last year, baseline parameters for the traveling-wave (TW) rf structures foreseen for each of the linacs have been determined. In the following, the methodology of the rf design and specific structures for positron, electron, and common linac are presented.

RF DESIGN METHODOLOGY

Large parameter spaces have to be considered when optimizing traveling-wave (TW) structures. In our case, one cell is characterized by its aperture radius (iris radius) a , iris thickness d , and synchronous rf phase advance ψ , where $L_c = \lambda\psi/(2\pi)$ is the cell length with the frequency $f = c/\lambda$. Structures are linearly tapered in aperture and iris thickness, such that 7 parameters describe one structure. To calculate millions of structures, cell parameter lookup tables and analytic formulas are used as far as possible.

* hermann.winrich.pommerenke@cern.ch

Cell Lookup Table

The general cell geometry (Fig. 2) is based on the Swiss-FEL C-band structure [3] and as such the lookup table database has been computed at its frequency of 5.712 GHz. However, this choice is arbitrary and it can be scaled to any frequency using appropriate proportionalities.

The lookup table contains over 200 reference geometries with different geometries ($0.08\lambda \leq a \leq 0.36\lambda$, $0.02\lambda \leq d \leq 0.19\lambda$, $2\pi/3 \leq \psi \leq 9\pi/10$). For each cell, iris ellipticity has been optimized for a maximum modified Poynting vector S_c [4] as small as possible. Rf parameters of the lowest higher-order modes (HOMs) have been numerically computed at the synchronous frequencies. The table contains frequencies, quality factors, shunt impedances, group velocities, and passband limits of the 20 lowest monopoles and dipoles each as well as high-gradient limits of the fundamental mode.

Analytic Formulas

The TW structures accelerate two bunches per rf pulse and thus profit from the widely-used SLED-type (SLAC energy doubler) rf pulse compressor [5]: A storage cavity with unloaded Q factor Q_c and coupling β is charged by the klystron. When the klystron phase is reversed, the storage cavity is discharged, adding to the klystron pulse. For a klystron pulse with arbitrary amplitude $A_k(t)$ (in units of \sqrt{W}), the amplitude into the TW structure is found to be

$$A_\ell(t) = A_k(t) - \alpha\mu e^{-\mu t} \int_0^t e^{\mu t'} A_k(t') dt', \quad (1)$$

where $\mu = \omega(1 + \beta)/2Q_c$ is the reciprocal storage cavity filling time and $\alpha = 2\beta/(1 + \beta)$. Assume now a rectangular klystron pulse of length T_k , amplitude $A_{k,0}$ and phase reversal at $t = T_k - T_f$, where T_f is the TW structure filling time. We obtain for $T_k - T_f \leq t \leq T_k$:

$$\frac{A_\ell(t)}{A_{k,0}} = 1 - \alpha \left(1 + \left[1 - 2e^{\mu(T_k - T_f)} \right] e^{-\mu[t - \tau(z)]} \right). \quad (2)$$

Following Ref. [6], the transient gradient during structure filling can be derived as

$$G(z, t) = A_\ell [t - \tau(z)] \sqrt{\omega \frac{\varrho(0)}{v_g(0)}} g(z), \quad (3)$$

where

$$g(z) = \sqrt{\frac{v_g(0)\varrho(z)}{v_g(z)\varrho(0)}} \exp \left[-\frac{\omega}{2} \int_0^z \frac{dz'}{v_g(z')Q(z')} \right] \quad (4)$$

Content from this work may be used under the terms of the CC BY 4.0 licence (© 2021). Any distribution of this work must maintain attribution to the author(s), title of the work, publisher, and DOI

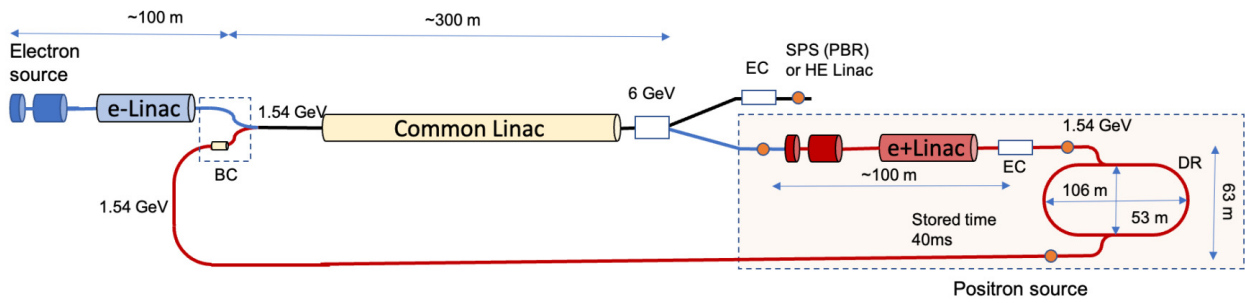


Figure 1: Latest baseline layout of the FCC-ee pre-injector complex [2].

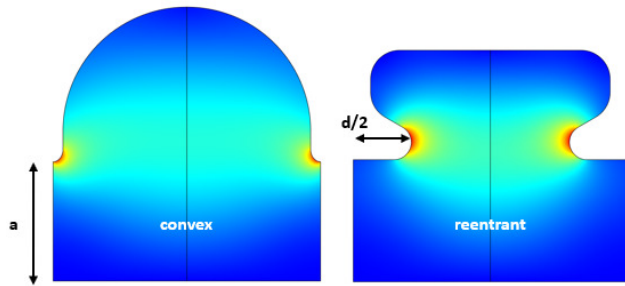


Figure 2: Basic geometry of reentrant and convex TW structure cells considered for the FCC-ee injector.

is the normalized steady-state gradient and $\rho \equiv R'/Q$, Q , v_g , and τ denote normalized shunt impedance per unit length, quality factor, group velocity, and signal time delay, respectively.

The long-range transverse wake function of the n -th dipole mode is computed in time domain from the frequency domain quantities as

$$W_{x,n}(s) = -2K_{x,n} \cdot F(\omega_n, \sigma_z) \cdot \exp\left(-\frac{\omega_n}{2Q_n} s/c\right) \cdot \sin(\omega_n s/c) \quad (5)$$

for $s = z - ct > 0$, where $K_{x,n} = (R'_x/Q)_n \omega_n^2 / (4c)$ is the dipole kick factor per unit structure length and unit beam offset (half of the wake amplitude). $F(\omega_n, \sigma_z) = \exp[-(\omega_n \sigma_z / c)^2]$ is the form factor for a gaussian bunch with rms length σ_z . Similar expressions are found for transverse wake function and dipole modes, respectively. The full wake of the structure can be approximated with good accuracy by summing the wake functions of each mode in each cell.

POSITRON LINAC

The rf design of the positron linac TW structure is strongly driven by frequency, aperture, length, as well as high-gradient and wake limits. Of secondary importance are e.g. klystron pulse length, rf pulse compressor parameters, but also mechanical constraints such as integration into the solenoid channel. Sweeps over large parameter spaces were carried out to find suitable structures fulfilling all these requirements (Fig. 3). The effective shunt

impedance $R_{\text{eff}} = \langle G(t = T_k) \rangle^2 L_s / P_k$ (squared voltage at injection per unit klystron power) is plotted against structure length.

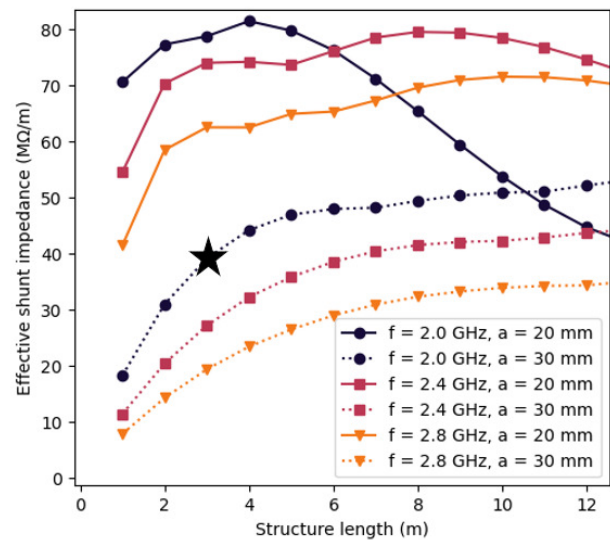


Figure 3: Sweep of TW structure parameters for positron linac. For each frequency, aperture, and length, the structure with highest effective shunt impedance is selected. The star marks the baseline structure "F3".

A 30 mm aperture radius will be necessary to transport the positron beam at low energies (10 000 mm mrad) with acceptable beam losses. Thus, a low frequency of 2.0 GHz and a reentrant cell geometry were chosen to reduce group velocity and achieve high effective shunt impedance with a reasonable structure length of 3 m. Further parameters of the TW structure called "F3" are listed in Table 1.

The long-range transverse wake (Fig. 5) is damped by detuning of dipole modes without additional damping elements. This is achieved by tapering the iris thickness alone since the aperture is constant. The structure can be safely operated with an average gradient (at beam injection) of $\langle G \rangle = 20$ MV/m, with maximum surface electric field and modified Poynting vector (Fig. 4) well below empirical limits.

The phase advance of $9\pi/10$ increases shunt impedance but also means that the rf pulse will suffer from dispersion.

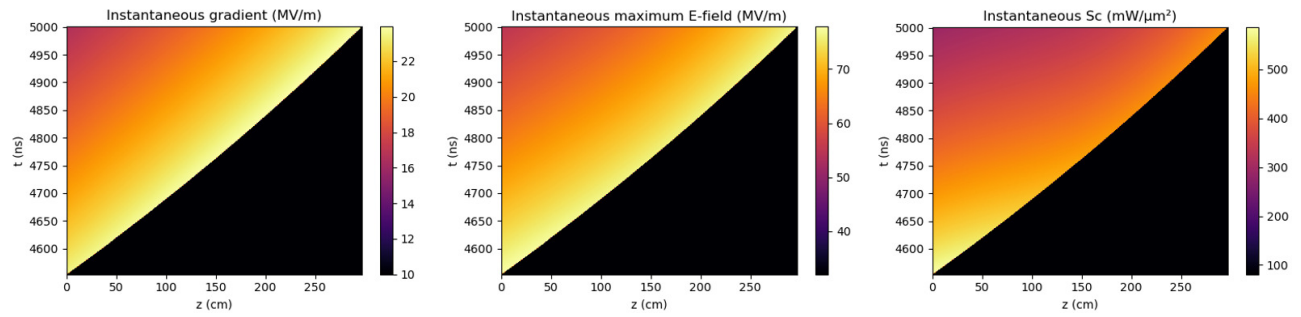


Figure 4: Instantaneous field amplitudes during the filling of positron linac TW structure.

Table 1: Structure parameters for positron linac.

Frequency	2.0 GHz
Constant aperture	30 mm
Rf phase advance	$9\pi/10$
Length (num cells)	3.0 m (44)
Tapered iris thickness	14.3 mm \rightarrow 20.0 mm
Transv. wake at 15 ns	0.17 V/pC/mm/m
Filling time	447 ns
SLED coupling	17
Eff. shunt impedance	39 M Ω /m
Average gradient	20 MV/m
Max. instant. E	77 MV/m
Max. instant. S_c	585 mW/ μm^2
Klystr. pulse length	5 μs

Table 2: Parameters for common and electron linac.

	Structure for both linacs	Alternative for e- linac
Frequency	2.8 GHz	2.0 GHz
Average aperture	0.15 λ	0.15 λ
Rf phase advance	$2\pi/3$	$5\pi/6$
Length (# cells)	3.0 m (84)	3.0 m (48)
Cell geometry	reentrant	reentrant
Transv. wake	0.2 V/pC/mm/m	0.1 V/pC/mm/m
Filling time	486 ns	884 ns
SLED coupling	15	14
Eff. shunt imp.	87 M Ω /m	66 M Ω /m
Average gradient	25 MV/m	25 MV/m
Max. instant. E	95 MV/m	100 MV/m
Max. instant. S_c	685 mW/ μm^2	737 mW/ μm^2
Klystr. pulse length	3 μs	5 μs

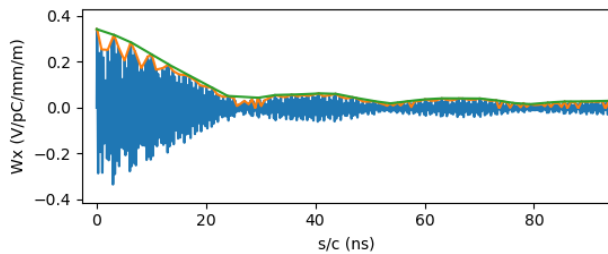


Figure 5: Transverse wake of positron linac TW structure.

This is acceptable since only two bunches are accelerated per pulse. If required, the dispersion can be compensated by modulating the klystron pulse.

ELECTRON AND COMMON LINAC

Electron and common linac feature more conventional structures whose choice is driven by overall long-range and short-range wakes and efficiency more than by the iris aperture. Table 2 shows parameters of two structures: (1) 2.8 GHz structure for the common linac that can also be used for the electron linac as a cost-efficient option, and (2) an alternative for the electron linac with lower frequency and larger aperture. Both structures fulfill the requirement of an action amplification less than 10 % for the given bunch parameters. Future studies will also consider a C-band option at 5.6 GHz which will have higher shunt impedance but also suffer from stronger wakes.

CONCLUSION

Baseline TW structures for each of the FCC-ee injector linacs have been designed. Large-aperture high-phase advance cavities will accelerate the high-emittance positron beam to 1.5 GeV, more conventional structures accelerate electrons and positrons after the damping ring up to 6 GeV. High-gradient and wakefield limitations have been taken into account as well.

For each linac, structure parameters have been optimized by scanning large parameter spaces. This has been facilitated by creating lookup tables and deriving analytic formulas.

The choice of parameters will be finalized during the upcoming months. If required, the rf design will be adjusted considering further beam dynamics results, mechanical integration into the lattice, and thermal simulations.

ACKNOWLEDGMENT

This project has received funding from the European Union's Horizon 2020 research and innovation programme under grant agreement No 951754. This work was also done under the auspices of CHART (Swiss Accelerator Research and Technology Collaboration).

REFERENCES

- [1] A. Abada *et al.*, “FCC-ee: The lepton collider,” *The European Physical Journal Special Topics*, vol. 228, no. 2, pp. 261–623, 2019, doi:10.1140/epjst/e2019-900045-4
- [2] P. Craievich *et al.*, “The fceee pre-injector complex,” in *13th International Particle Accelerator Conference (IPAC2022), Bangkok, Thailand*, vol. IPAC2022, 2022, pp. 2007–2010, doi:10.18429/JACoW-IPAC2022-WEPOPT063
- [3] J.-Y. Raguin and M. Bopp, “The SwissFEL C-band accelerating structure: RF design and thermal analysis,” in *26th Linear Accelerator Conference (LINAC2012), Tel-Aviv, Israel*, 2012, pp. 501–503, <https://accelconf.web.cern.ch/linac2012/papers/tupb012.pdf>
- [4] A. Grudiev, S. Calatroni, and W. Wuensch, “New local field quantity describing the high gradient limit of accelerating structures,” *Physical Review Accelerators and Beams*, vol. 12, no. 10, 2009, doi:10.1103/physrevstab.12.102001
- [5] Z. D. Farkas, H. A. Hoag, G. A. Loew, and P. B. Wilson, “SLED: A method of doubling SLAC’s energy,” in *9th International Conference on High-Energy Accelerators (HEACC1974)*, 1974, pp. 576–583.
- [6] A. Lunin, V. Yakovlev, and A. Grudiev, “Analytical solutions for transient and steady state beam loading in arbitrary traveling wave accelerating structures,” *Physical Review Special Topics - Accelerators and Beams*, vol. 14, no. 5, 2011, doi:10.1103/physrevstab.14.052001